Prediction of Roof Collapse for Rectangular Underground Openings

A M Suchowerska[1], J P Hambleton[2] and J P Carter[3]

ABSTRACT

In order to effectively predict the roof collapse of underground openings using continuum models, it is imperative that a realistic failure criterion is used to represent the rock mass. However, for coal mining operations, there is still uncertainty as to the appropriate failure criterion that should be used for the coal measure strata. This study compares stability numbers and collapse mechanisms for a rectangular underground opening predicted based on three commonly used failure criteria: the standard Mohr-Coulomb, Mohr-Coulomb with a tension cut-off and Hoek-Brown. Three methods of analysis are considered:

1. an analytical upper bound method
2. an upper and lower bound finite element formulation
3. the displacement finite element method.

The theoretical results are also compared with field measurements of subsidence above longwall coal mining. For the standard Mohr-Coulomb failure criterion, the friction angle governs the shape of the collapse mechanism, and the so-called critical width (the cavity width above which failures extend to the ground surface) ascertained from field observations in the New South Wales coalfields corresponds to a friction angle of approximately 30°. On the other hand, predictions obtained based on the Hoek-Brown failure criterion consistently overestimate the critical width. The results also show that tensile failure governs the stability of the cavity and shape of the collapse mechanism when a tension cut-off is introduced for the Mohr-Coulomb yield criterion.

INTRODUCTION

In coal mining operations, most forms of roof collapse are undesirable (eg collapse of the roof above a roadway), although some are expected (eg the collapse of the overburden above a longwall panel). For both cases, mine designers need to be able to predict if and how the failure will occur.

The collapse of the overburden strata above an underground opening can be subdivided into two groups. So-called subcritical failures are contained entirely within the overburden height. They typically occur when the width of the cavity (W) relative to the height of the overburden (H) is small (see shape in Figure 1a). In this case, there is sufficient overburden thickness to generate a pressure arch acting through the rock mass, which supports the overlying material and usually leads to reduced subsidence of the ground surface.

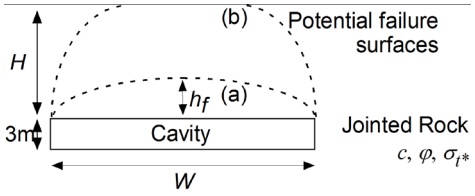

FIG 1 – Roof collapse for a rectangular cavity.

So-called supercritical failures extend through the entire overburden (see shape in Figure 1b). They occur when the width of the cavity relative to the height of the overburden is large. In Australian coalfields, many failures are supercritical since coal seams are located at relatively shallow depths.

In the latter half of the 20th century, the stability of underground cavities was usually assessed using empirical methods. Empirical data compiled from field observations were used to develop tunnel support design methods based on rock mass classification systems, *viz*, the rock mass rating (RMR) (Bieniawski, 1973) and the Q index (Barton, Lein and Lunde, 1974). Lang (1994) presented a detailed empirical stability chart relating the RMR to cavity span, which was then further refined by Ouchi *et al* (2004) for cavities in lower-quality rock masses. In general, there were uncertainties on the boundary of the zone of stability because of the large variations in data. Also, a significant drawback in using these empirical methods is that stability is correlated with rock mass classification coefficients RMR or Q, which must be regarded as indices rather than fundamental rock mass properties.

Numerical modelling has become widely used in industry as a means of assessing cavity stability. A common assumption in geotechnical stability analysis is to regard the rock mass as

1. SAusIMM, PhD Candidate, Centre for Geotechnical and Materials Modelling, The University of Newcastle, Faculty of Engineering and Built Environment, Building EA, Callaghan NSW 2308. Email: anastasia.suchowerska@uon.edu.au
2. Research Academic, Centre for Geotechnical and Materials Modelling, The University of Newcastle, Callaghan NSW 2308. Email: james.hambleton@newcastle.edu.au
3. Emeritus Professor, Centre for Geotechnical and Materials Modelling, The University of Newcastle, Callaghan NSW 2308. Email: john.carter@newcastle.edu.au

a continuum. In this approach, the strength of the rock mass is prescribed according to a failure criterion that attempts to account for the strength of both the discontinuities and the intact rock. The Mohr-Coulomb and the Hoek-Brown failure criteria are most commonly assumed.

The aim of this paper is to compare stability numbers and collapse mechanisms for rectangular underground openings deforming under plane strain conditions predicted based on the Mohr-Coulomb and Hoek-Brown failure criteria. While the results can be applied to various types of rectangular underground openings, the focus of this study is on longwall coal mining, where a primary concern is the stability of roadways and longwall panels. As the stability of rectangular underground openings assuming the Hoek-Brown failure criterion was considered previously by the authors (Suchowerska *et al*, 2011; Suchowerska, 2014), this paper concentrates mainly on results obtained based on the Mohr-Coulomb yield criterion, with and without a tension cut-off. Stability numbers and collapse mechanisms are evaluated based on an analytical upper bound method, upper and lower bound finite element formulations and the displacement finite element method. The theoretical results are also compared with field measurements of subsidence above longwall coal mining.

PROBLEM DEFINITION

The stability problem considered in this paper is depicted in Figure 1. Plain strain is assumed, and the rock mass is considered to behave as a perfectly plastic material obeying the Mohr-Coulomb yield criterion and associated plastic flow (*cf* Chen, 1975). This model is the same as was used in the previous analysis based on the Hoek-Brown failure criterion (Suchowerska *et al*, 2011) and can be regarded as an idealised representation of an underground cavity where the overlying material is reasonably uniform.

In the Mohr-Coulomb failure criterion, the shear stress at failure (τ) is governed by the cohesion (c) and friction angle (φ) of the material, as well as the normal stress (σ_n) acting on the failure plane, as follows:

$$\tau = c + \sigma_n \tan\varphi \quad (1)$$

where compression is considered positive.

Figure 2a shows the Mohr-Coulomb failure criterion in the shear stress-normal stress plane and also the principal stress plane (Brady and Brown, 1992). The tensile strength of the material (σ_t) according to the Mohr-Coulomb criterion is given by $\sigma_t = 2c\cos\varphi/(1+\sin\varphi) = \sigma_c(1-\sin\varphi)/(1+\sin\varphi)$, where σ_c is the uniaxial compressive stress of the material defined as $\sigma_c = 2c\cos\varphi/(1-\sin\varphi)$. In principal stress space, the criterion may be expressed as:

$$\sigma_1 = N_\varphi \sigma_3 + 2c\sqrt{N_\varphi} \quad (2)$$

where:

σ_1 and σ_3 are the major and minor principal stresses respectively

$N_\varphi = (1+\sin\varphi)/(1-\sin\varphi)$

There have been numerous proposals for methods of implementing a tension cut-off to the Mohr-Coulomb failure criterion (Chen and Saleeb, 1982), and only the most common form is considered here. The tension cut-off is applied as shown in Figure 2b by prescribing a value of maximum tensile stress of the rock mass, denoted by σ_{t^*}. This method effectively truncates the Mohr-Coulomb failure criterion.

The range of values for the variables assumed in the study is presented in Table 1. The values of the friction angle φ were selected to be representative of sedimentary strata (Goodman, 1989). The values of the ratio W/H were varied from one to four to encompass both small and wide cavities.

METHODS OF ANALYSIS

Three different computational techniques were used in this study. The first method involved application of upper bound (UB) and lower bound (LB) finite element limit analysis (Lyamin and Sloan, 2002a, 2002b; Krabbenhoft *et al*, 2005). The Mohr-Coulomb failure criterion with and without a tension cut-off was considered using this first method. The second

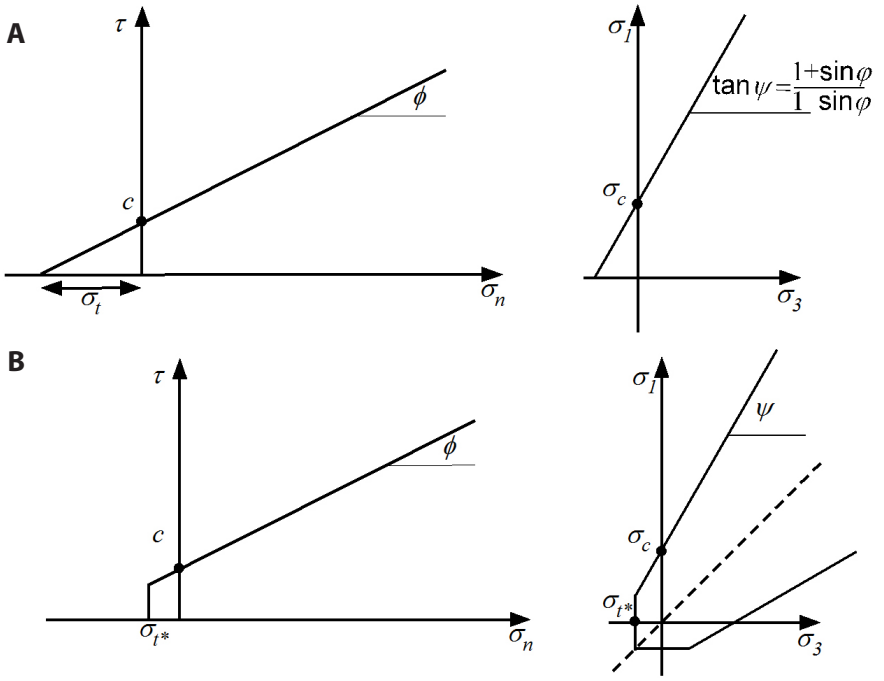

FIG 2 – Schematic representation of (A) a standard Mohr-Coulomb failure criterion (adapted from Brady and Brown, 1992); (B) a Mohr-Coulomb failure criterion with a tension cut-off (adapted from Chen and Saleeb, 1982; Clausen and Damkilde, 2006).

TABLE 1
Variables considered in the analysis of cavity roof collapse using the Mohr-Coulomb failure criterion.

Variable	Description	Values considered
H	Overburden thickness (cover depth)	10 m to 40 m, increments of 10 m
W	Width of rectangular cavity	10 m to 40 m, increments of 10 m
γ	Unit weight of material	N/A
φ	Friction angle of overburden rock mass	20° to 50°, increments of 10°
c	Cohesion of overburden rock mass	1.5 MPa
σ_{t^*}	Tensile strength	σ_t to 0.03 σ_t

method was the analytical closed form UB analysis proposed by Fraldi and Guarracino (2009). This approach considered only the standard Mohr-Coulomb failure criterion. The third method is the displacement finite element method, where a tension cut-off was again considered. Additional details regarding these methods can be found in the complementary paper by the authors (Suchowerska *et al*, 2011).

For any given cavity geometry (W, H) and mechanical properties of the rock mass (c, φ), the objective of the analysis is to determine the unit weight corresponding to collapse and the corresponding failure mechanism. The unit weight required to induce collapse, denoted by γ^*, can be related to the true unit weight (γ) by $\gamma^* = \gamma F$, where F is regarded as the factor of safety. For $F > 1$, the configuration is predicted to be stable, and for $F < 1$, the configuration is predicted to be unstable. The case $F = 1$ corresponds to incipient collapse. The stability numbers N and Q are used as a convenient means of presenting the results in a non-dimensional form. These are defined as follows:

$$N = \frac{\sigma_c}{\gamma W F} \quad , \quad Q = \frac{c}{\gamma W F} \tag{3}$$

While N and Q are essentially equivalent, the quantity Q is useful for isolating the effects of varying φ since the compressive strength σ_c appearing in the definition of N also varies with φ.

Finite element upper and lower bound formulation

Rigourous bounds on the stability numbers were obtained using the numerical techniques developed by Lyamin and Sloan (2002a, 2002b) and Krabbenhoft *et al* (2005). Limit analysis involves bracketing the true theoretical collapse load (stability number) between an upper bound and a lower bound. The true collapse load can be approximated well if the difference between the UB and LB is small.

The tension cut-off, as the second form of the Mohr-Coulomb failure criterion considered in this paper, was implemented in the limit analysis algorithms by prescribing an additional failure surface. This additional failure surface was defined using a cohesion with a value given by $c = \sigma_{t^*}$ and a friction angle of $\varphi = 90°$. The minimum number of elements adopted in each analysis was made large enough to ensure a maximum margin of ten per cent between the UB and LB predictions of the collapse load.

Closed form upper bound analysis

There have been several derivations of upper bound solutions for an underground rectangular cavity that consider the Mohr-Coulomb failure criterion (Lippmann, 1971; Nunziante, Gesualdo and Minutolo, 2001). The upper bound solution developed by Fraldi and Guarracino (2009) assumes the following failure criterion:

$$\tau = \pm A\sigma_{ci}\left(\frac{\sigma_n - \sigma_t}{\sigma_{ci}}\right)^B \tag{4}$$

where:

σ_{ci} is the uniaxial compressive strength of the intact rock
σ_t is the maximum tensile strength of the rock mass
A and B are dimensionless parameters

The original analysis by Fraldi and Guarracino (2009) was completed for a rectangular cavity in a Hoek-Brown material. However, their solution also applies to the Mohr-Coulomb criterion by selecting $A = \tan\varphi$, $B = 1$ and $\sigma_t = c\cot\varphi$. The limitation of this method is that it only considers subcritical failure. The following equation gives the critical width ratio $(W/H)_{crit}$ at which the collapsing block height (h_f) (see Figure 1) equals the overburden thickness (H):

$$\left(\frac{W}{H}\right)_{crit} = \frac{2AB^{-B}(1+B)^B\sigma_{ci}^{(1-B)}\sigma_t^B B}{(1+B)\sigma_t} \tag{5}$$

The complete derivation of Equation 5 was presented in a previous paper by the authors (Suchowerska *et al*, 2011). The predictions of this method are compared with other approaches utilised in this paper.

Displacement finite element modelling

Numerical modelling was also conducted using the commercial software Abaqus, which is based on the displacement finite element method. The modelling consisted of the same two-step process as used in the complementary paper by the authors (Suchowerska *et al*, 2011). In the first analysis step, the geostatic forces were equilibrated, and in the second analysis step, a rectangular section of material was removed as a single block excavation and the internal stresses in the rock mass were allowed to come to equilibrium. The Mohr-Coulomb failure criterion with a tension cut-off was incorporated into the constitutive model representing the rock mass using the formulation developed by Clausen and Damkilde (2006).

In this type of analysis, the collapse load was defined as the unit weight at which overall equilibrium of the model could just be obtained. The point of incipient collapse was also confirmed by reviewing the shape and magnitude of the displacement curve at the midpoint on the roof of the cavity. The analyses were conducted for an overburden depth of $H = 150$ m.

RESULTS

Standard Mohr-Coulomb failure criterion

The results for the standard Mohr-Coulomb failure criterion are presented in terms of the stability factors N and Q in Figure 3. In general, the larger magnitudes of the friction angle φ gave larger values of N. This prediction indicates that materials with larger friction angles would, in general, be less stable. This initial observation seems counterintuitive, but this trend arises because the magnitude of σ_c is also influenced by φ. In contrast, the larger magnitudes of the friction angle gave smaller predicted values of Q. The curve for $\varphi = 20°$ is truncated at both small and large values of the ratio W/H as the predicted failure did not correspond to the roof collapse

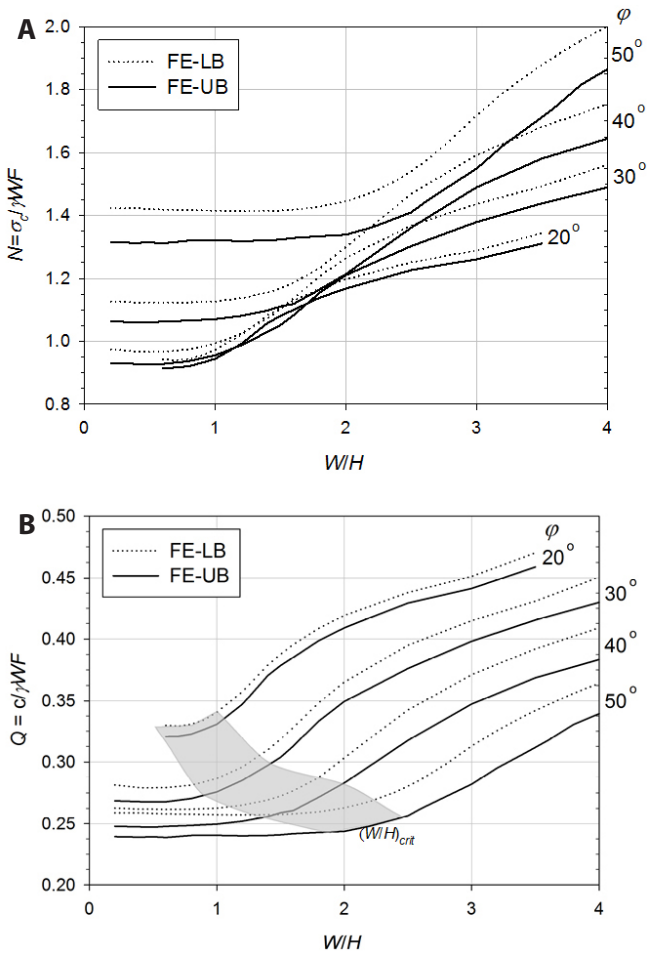

FIG 3 – Stability charts based on finite element upper bound and finite element lower bound limit analysis formulations for (A) stability factor *N* and (B) stability factor *Q*.

mechanism, which is schematically defined in Figure 1. The predicted failure mechanisms for $\varphi = 20°$ when $W/H < 0.6$ and $W/H > 3.5$ are discussed by Suchowerska (2014).

The distinction between supercritical and subcritical failure was exhibited as two different portions of the curve on the stability charts, which overall appears to consist of three portions in Figure 3. The portion of the curve at low values of the ratio W/H, where the curve is approximately horizontal, corresponds to the failure surface remaining within the overburden. An example of this subcritical failure is depicted in Figure 4a, where plastic energy dissipation is plotted for $W/H = 0.5$ and $\varphi = 30°$. Another portion of the curve, at large values of ratio W/H, involves the predicted failure surface extending through the overburden. An example of this supercritical failure is depicted in Figure 4b, which shows plastic energy dissipation for $W/H = 3$ and $\varphi = 30°$. The third portion of the curve is located in between the two portions mentioned previously. This middle portion corresponds to the failure surface transitioning from subcritical to supercritical, as shown in Figure 5. Typical failure surfaces have been marked on the plots of plastic energy dissipation as dashed lines. There does not appear to be a distinct position along the curve that can be easily marked as the boundary of subcritical and supercritical failure. The grey region in Figure 3b shows the range corresponding to the transition zone for all the friction angles considered here.

The boundaries between the various portions on the curve occur at different magnitudes of the ratio W/H for each of the curves of varying friction angle φ (Figure 3b). The reason for this can be understood by comparing the plastic energy dissipation for a range of friction angles for $W/H = 3.0$ (Figure 6). In these cases of supercritical failure, it can be seen that the angle between the failure surface and vertical (θ) appears to be approximately equal to the friction angle of the rock mass. Therefore, materials with larger friction angles predict a flatter profile for the failure surface. This finding is in agreement with the analyses of the Terzaghi trap-door problem (eg Smith, 1998).

The results for the analytical upper bound solution of Fraldi and Guarracino (2009) (CF-UB) for subcritical failure are presented in Figure 7a. The stability parameter N increases as the friction angle φ increases. The dashed line shows the limit when the failure surface extends through the entire overburden thickness. This limit was determined using Equation 5.

The CF-UB results are in reasonable agreement with those predicted by finite element limit analysis (Figure 7b). The CF-UB curves for the friction angles $\varphi = 40°$ and 50° plot within the upper and lower bounds. However, the CF-UB curves do not remain within the bounds at larger magnitudes of ratio W/H. This is probably because the CF-UB method assumes that the remaining strata, left behind after the roof has collapsed, will be stable. This is unlikely as the thickness of the collapsing block h_f approaches the full overburden thickness H. For $\varphi = 30°$, CF-UB results are consistently outside the bound from finite element limit analysis. In this case, the mechanism assumed for the CF-UB solution is not able to match the most critical shape. Given that the analytical solution was developed for the Hoek-Brown failure criterion,

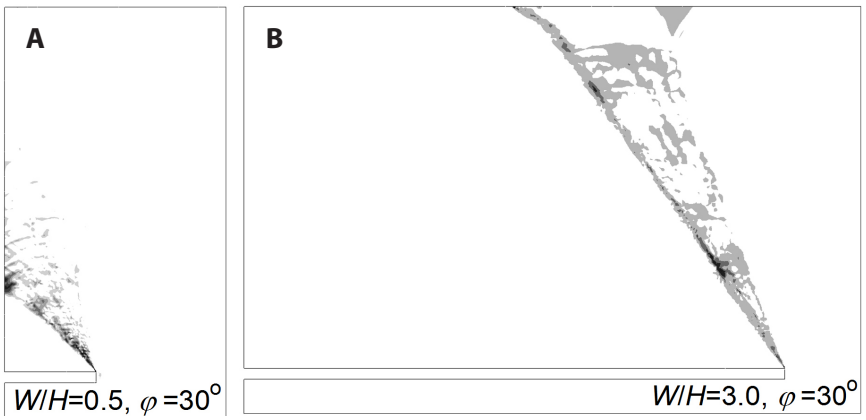

FIG 4 – Finite element lower bound predictions of the degree of plastic dissipation, showing that the failure surfaces are (A) subcritical for low values of the ratio *W/H* and (B) supercritical for high values of the ratio *W/H*.

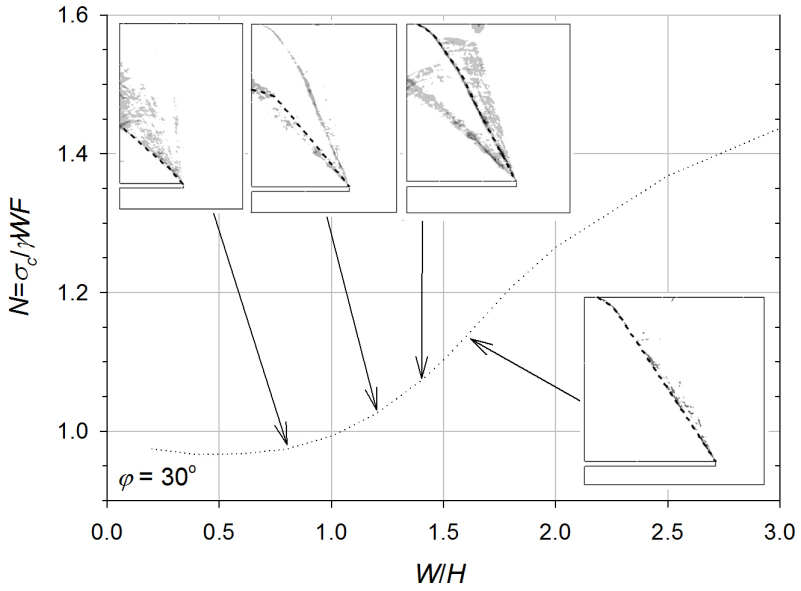

FIG 5 – Finite element upper bound predictions of the degree of plastic dissipation, with approximate locations of the failure surfaces shown as dashed lines. There is a progressive transition from subcritical to supercritical failure mechanisms for increasing ratio W/H.

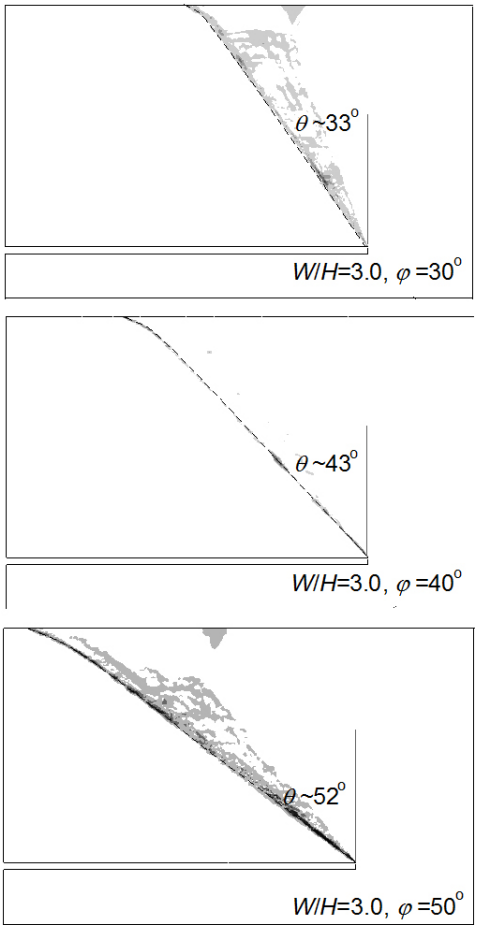

FIG 6 – Finite element upper bound predictions of the degree of plastic dissipation for $W/H = 3.0$ and varying friction angle φ.

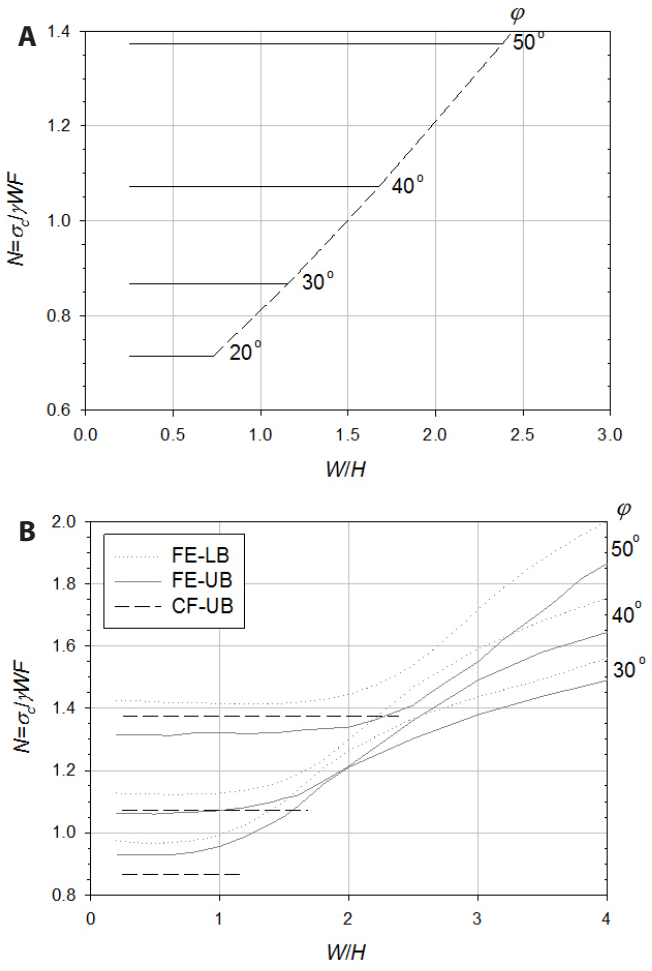

FIG 7 – Stability chart for standard Mohr-Coulomb criterion: (A) closed form upper bound (CF-UB) analysis; (B) comparison between predictions obtained from CF-UB, finite element upper bound (FE-UB) and finite element lower bound (FE-LB) limit analysis.

which corresponds to relatively high friction angles in regions of tensile and low confining stress, the equation selected to represent the failure surface would necessarily correspond to a smaller inclination of the failure surface from the horizontal. This assumed mechanism is unable to match the large inclination of the failure surface observed when the friction angle is low.

Mohr-Coulomb with tension cut-off

Figure 8 shows the results from the finite element limit analyses when the tensile strength σ_{t^*} is included in the Mohr-

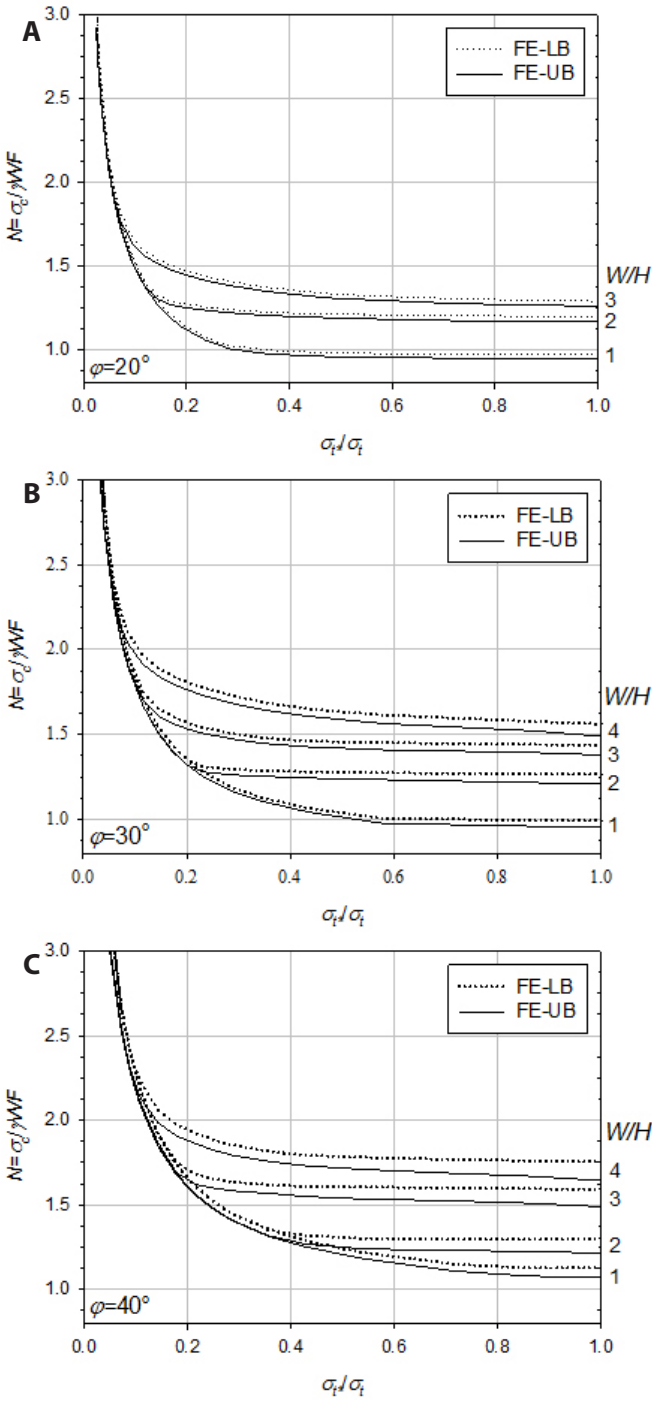

FIG 8 – Stability charts obtained using finite element upper bound (FE-UB) and finite element lower bound (FE-LB) limit analysis for a range of normalised tensile strengths (σ_{t^*}/σ_t): (A) $\varphi = 20°$; (B) $\varphi = 30°$ and (C) $\varphi = 40°$.

Coulomb failure criterion for friction angles φ = 20°, 30° and 40°. The results for the stability number N have been plotted against the ratio of the imposed tensile strength σ_{t^*} and the tensile capacity predicted by the standard Mohr-Coulomb failure criterion σ_t. Over the range of W/H considered, the stability number N remains relatively constant at large values of the ratio σ_{t^*}/σ_t. At lower magnitudes of σ_{t^*}/σ_t, the individual curves corresponding to the different values of W/H combine to plot as a single curve. This curve asymptotically approaches zero as the stability parameter N tends to infinity.

The results presented in Figure 8 clearly show that, irrespective of the magnitude of other strength parameters, inclusion of a tensile cut-off in the Mohr-Coulomb failure criterion will govern the stability of the cavity. In the most extreme case considered, where σ_{t^*}/σ_t = 0.028, failure in the overburden is located primarily in the area close to the cavity roof (Figure 9). The failure surface appears to be relatively flat, and separation under tension is the primary mode of failure. The failure surface for magnitudes of the ratio σ_{t^*}/σ_t greater than 0.5 are all quite similar to the shape obtained when using the Mohr-Coulomb criterion with no tension cut-off, where shearing is the mode of failure.

Figure 10 presents the stability numbers assessed using the displacement finite element method. The results are in good agreement with the predictions obtained from finite element limit analysis, lying closer to the predicted lower bounds than the upper bounds.

DISCUSSION

The results from finite element limit analysis assuming the standard Mohr-Coulomb failure criterion show that the friction angle governs the shape of the failure surface. This response has also been observed when analysing the trapdoor problem (Davis, 1968; Smith, 1998). As a result, larger magnitudes of friction angle lead to larger values of the critical ratio $(W/H)_{crit}$. For the standard Mohr-Coulomb failure criterion with friction angles between 20° and 50°, the predicted critical ratio $(W/H)_{crit}$ ranged from 0.5 to 2.5. Previous studies conducted by the authors showed that the Hoek-Brown criterion predicted critical ratio $(W/H)_{crit}$ ranging from 1.5 to 8.0 for m_i values of 5–30 (Suchowerska *et al*, 2011), where m_i corresponds to an intact rock constant (Hoek, Carranza-Torres and Corkum, 2002). The stability chart for the Hoek-Brown failure criterion with m_i = 20 is presented in Figure 11, which is indicative of the results obtained for other magnitudes of m_i.

Stability numbers based on the Hoek-Brown and Mohr-Coulomb failure criteria are presented on a common chart in Figure 12. This comparison of results highlights the sensitivity of the stability number (and underlying collapse mechanism) to the assumed failure criterion for the rock mass. The magnitudes of the critical width ratio $(W/H)_{crit}$ were all significantly higher for the Hoek-Brown failure criterion than for the standard Mohr-Coulomb failure criterion. This can be explained by recognising that the Hoek-Brown failure criterion corresponds to effectively high friction angles in the range of tensile and very low confining stresses occurring in the strata above underground openings. As the effective friction angle increases, the critical width ratio $(W/H)_{crit}$ also increases.

The magnitudes of the stability factors N for the standard Mohr-Coulomb failure criterion are all much lower than for the Hoek-Brown failure criterion (Figure 12). From a practical perspective, this implies that the standard Mohr-Coulomb criterion predicts that the underground opening remains stable at much smaller magnitudes of σ_c for given magnitudes of γ, W and F than predicted using the Hoek-Brown failure criterion. This prediction of apparently greater stability when using the Mohr-Coulomb failure criterion possibly arises because of the much larger tensile capacity associated with the standard Mohr-Coulomb criterion relative to the Hoek-Brown criterion. Inclusion of a tension cut-off in the Mohr-Coulomb failure criterion increases the magnitude of the stability factor N, which predicts a less stable configuration. Further investigation is required to identify which failure criterion predicts roof collapse of an underground excavation in coal measure strata more accurately.

Field subsidence measurements have identified that the critical cavity width $(W/H)_{crit}$ in coal measure strata ranges

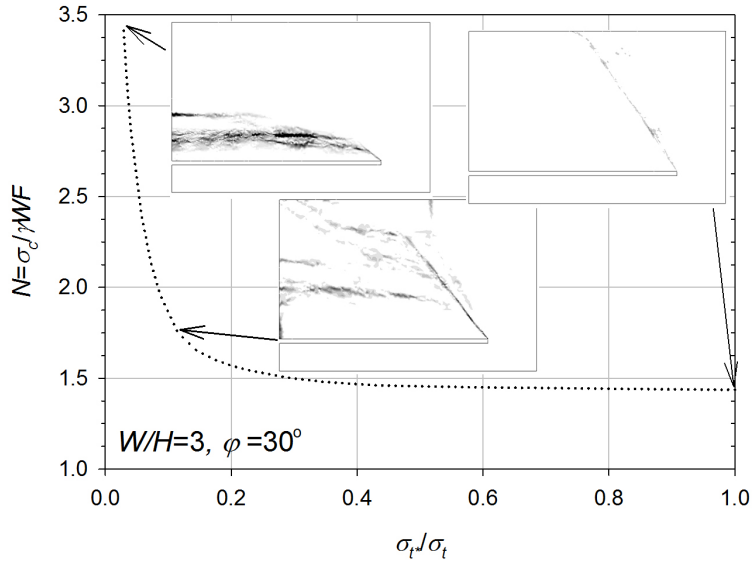

FIG 9 – Finite element upper bound predictions of the degree of plastic dissipation for a range of normalised tensile strengths (σ_{t^*}/σ_t).

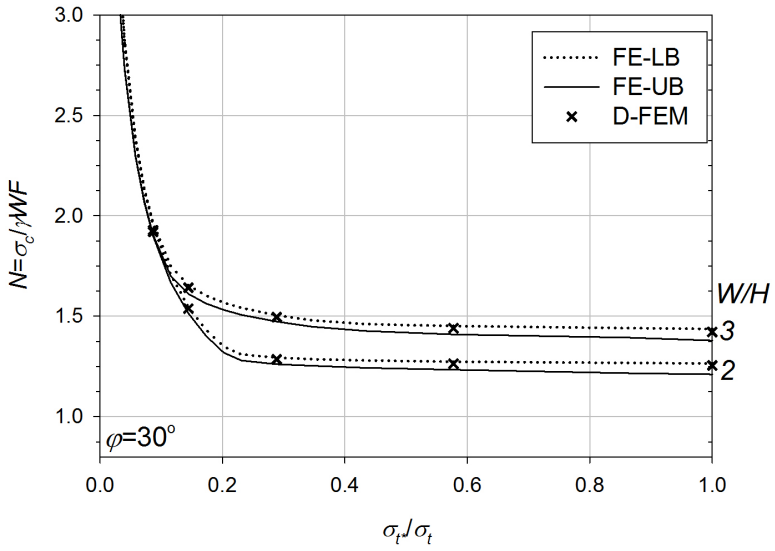

FIG 10 – Stability chart comparing results from upper and lower bound finite element limit analysis (FE-UB and FE-LB) with those based on the displacement finite element method (D-FEM).

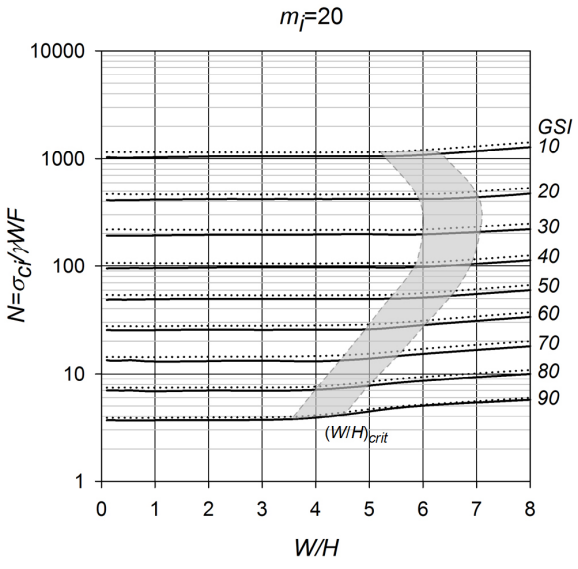

FIG 11 – Stability chart based on the Hoek-Brown failure criterion and finite element limit analysis (Suchowerska *et al*, 2011). The solid lines show upper bound and dotted lines show lower bound.

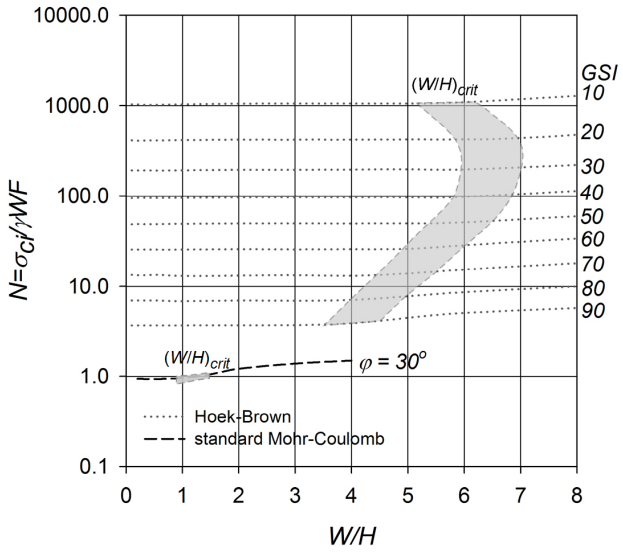

FIG 12 – Comparison of stability factors for the Hoek-Brown criterion and the Mohr-Coulomb failure criteria based on upper bound finite element limit analysis.

roughly from 1.0 to 1.6 in Australian coalfields (McNally *et al*, 1996; Mine Subsidence Engineering Consultants, 2007; Mills, 2009). This range of critical cavity widths is predicted by a friction angle of approximately 30° in the standard Mohr-Coulomb criterion. A similar value has been used in practical examples when representing the coal measure rock mass as a smeared homogeneous material (Coulthard and Holt, 2008; Seedsman, 2013).

The results presented here highlight the versatile and robust nature of finite element limit analysis relative to the analytical method and the displacement finite element method. The dependence of the shape of the failure surface on the friction angle might otherwise have been overlooked if only a limit equilibrium method was used as it requires a failure surface to be assumed. Finite element limit analysis is flexible enough to find the critical shape of the failure surface, and it is considerably less computationally intensive compared to the displacement finite element method.

CONCLUSIONS

This study has compared stability numbers and collapse mechanisms for a rectangular underground opening predicted based on three commonly used failure criteria: standard Mohr-Coulomb, Mohr-Coulomb with a tension cut-off and Hoek-Brown. The analytical upper bound method and displacement finite element method agreed with the predictions determined using the finite element upper and lower bound formulation.

For the Mohr-Coulomb failure criterion, the friction angle was shown to govern the shape of the failure surface, and subsequently the critical ratio $(W/H)_{crit}$. Larger friction angles led to larger values of the critical ratio $(W/H)_{crit}$. The Hoek-Brown criterion, which corresponds to effectively high friction angle in the presence of tensile and very low confining stress, predicts larger critical cavity width than the Mohr-Coulomb failure criterion. Stability numbers for both forms of the Mohr-Coulomb failure criterion were much lower than for the Hoek-Brown failure criterion. The results obtained by imposing a tension cut-off clearly show that the stability of the cavity and mechanism of failure of the overburden are controlled mainly by the tensile strength. The predictions of the normalised critical cavity width obtained with a friction angle of approximately 30° were the best match with field measurements.

REFERENCES

Barton, N R, Lein, R and Lunde, J, 1974. Engineering classification of rock masses for the design of tunnel support, *Rock Mechanics*, 6:189–239.

Bieniawski, Z T, 1973. Engineering classification of jointed rock masses, *Trans South African Institute of Civil Engineers*, 15:335–344.

Brady, B H G and Brown, E T, 1992. *Rock Mechanics for Underground Mining* (Chapman and Hall).

Chen, W-F, 1975. *Limit Analysis and Soil Plasticity* (Elsevier: Amsterdam).

Chen, W-F and Saleeb, A F, 1982. *Constitutive Equations for Engineering Materials* (John Wiley and Sons, Inc).

Clausen, J and Damkilde, L, 2006. A simple and efficient FEM-implementation of the Modified Mohr-Coulomb criterion, in *Proceedings 19th Nordic Seminar on Computational Mechanics*.

Coulthard, M A and Holt, G E, 2008. Numerical modelling of mining near and beneath tailings dam, in *Proceedings Southern Hemisphere International Rock Mechanics Symposium* (Australian Centre for Geomechanics: Perth).

Davis, E H, 1968. Theories of plasticity and the failure of soil masses, *Soil Mechanics, Selected Topics*, 341–380.

Fraldi, M and Guarracino, F, 2009. Limit analysis of collapse mechanisms in cavities and tunnels according to Hoek-Brown failure criterion, *International Journal of Rock Mechanics and Mining Sciences*, 46:665–673.

Goodman, R E, 1989. *Introduction to Rock Mechanics*, 576 p (John Wiley and Sons: New York).

Hoek, E, Carranza-Torres, C and Corkum, B, 2002. Hoek-Brown failure criterion – 2002 edition, in *Proceedings North American Rock Mechanics Society Meeting*, pp 267–273 (Rocscience: Toronto).

Krabbenhoft, K, Lyamin, A V et al, 2005. A new discontinuous upper bound limit analysis, I*nternational Journal for Numerical Methods in Engineering*, 63:1069–1088.

Lang, B D A, 1994. Span design for entry type excavations, Masters thesis (unpublished), The University of British Columbia, Vancouver.

Lippmann, H, 1971. Plasticity in rock mechanics, *International Journal of Mechanical Sciences*, 13:291–297.

Lyamin, A V and Sloan, S W, 2002a. Lower bound limit analysis using non-linear programming, *International Journal for Numerical and Analytical Methods in Geomechanics*, 26(2):181–216.

Lyamin, A V and Sloan, S W, 2002b. Upper bound limit analysis using linear finite elements and non-linear programming, *International Journal for Numerical Methods in Engineering*, 55(5):573–611.

McNally, G H, Willey, P L et al. 1996. Geological factors influencing longwall-induced subsidence, in *Proceedings Symposium on Geology in Longwall Mining*.

Mills, K W, 2009. Subsidence engineering, in *Australasian Coal Mining Practice*, third edition, pp 874–902 (The Australasian Institute of Mining and Metallurgy: Melbourne).

Mine Subsidence Engineering Consultants, 2007. General discussion on systematic and non systematic mine subsidence ground movements.

Nunziante, L, Gesualdo, A and Minutolo, V, 2001. Failure in Mohr-Coulomb soil cavities, *Canadian Geotechnical Journal*, 38:1314–1320.

Ouchi, A M, Pakalnis, R, et al. 2004. Update of span design curve for weak rock masses, presented at AGM 2004.

Seedsman, R, 2013. Practical strength criterion for coal mine roof support design in laminated soft rocks, *Mining Technology*, 122(4):243–249.

Smith, C C, 1998. Limit loads for an anchor/trapdoor embedded in an associative coulomb soil, *International Journal for Numerical and Analytical Methods in Geomechanics*, 22:855–865.

Suchowerska, A M, 2014. Geomechanics of single-seam and multi-seam longwall coal mining, PhD thesis (unpublished), University of Newcastle.

Suchowerska, A M, Merifield, R S, Carter, J P and Clausen, J, 2011. Prediction of underground cavity roof collapse using the Hoek-Brown failure criterion, *Computers and Geotechnics*, 44:93–103.